

Metallic versus insulating behavior in the A-site ordered perovskite oxides $ACu_3Co_4O_{12}$ ($A = Ca$ and Y) controlled by Mott and Zhang-Rice physics

Takashi Mizokawa,¹ Yosuke Morita,¹ Takaaki Sudayama,¹ Kou Takubo,¹ Ikuya Yamada,² Masaki Azuma,² Mikio Takano,² and Yuichi Shimakawa²

¹*Department of Physics and Department of Complexity Science and Engineering, University of Tokyo, Kashiwa, Chiba 277-8561, Japan*

²*Institute for Chemical Research, Kyoto University, Uji, Kyoto 611-0011, Japan*

(Received 13 May 2009; revised manuscript received 26 July 2009; published 8 September 2009)

We report on a photoemission study of A-site ordered perovskite oxides $ACu_3Co_4O_{12}$ ($A = Ca$ and Y) which are metallic for $A = Ca$ and insulating for $A = Y$. If the Cu valence is +2 as stabilized by the square planar coordination, the Co valence for $A = Ca$ is formally +4 and the system could be a Mott insulator while that for $A = Y$ should be +3.75 and the system is a doped Mott insulator. The photoemission study reveals that the Cu valence for $A = Ca$ and Y is formally +3 with the d^9L configuration (L : an O $2p$ hole) which corresponds to the Zhang-Rice singlet state. In addition, it is found that the Co valence for $A = Y$ is formally +3 with the low-spin d^6 configuration consistent with its insulating behavior.

DOI: [10.1103/PhysRevB.80.125105](https://doi.org/10.1103/PhysRevB.80.125105)

PACS number(s): 71.30.+h, 79.60.-i, 71.28.+d

I. INTRODUCTION

Transition-metal oxides with perovskite structure ABO_3 show various physical properties of interest including superconductivity, colossal magnetoresistance, metal-insulator transitions, and multiferroic behaviors.¹ The B site of the perovskite structure is highly flexible and allows various lattice distortions such as the tilting, elongation, and compression of the BO_6 octahedron.² In A-site ordered perovskite $ACu_3B_4O_{12}$, the three quarters of A sites are occupied by Cu ions and the BO_6 octahedra are tilted to stabilize the Cu ions with the pseudosquare planar coordination. In A-site ordered perovskite oxides, the Cu^{2+} ions tend to be stabilized by the square planar coordination.

Recently, various A-site ordered perovskite oxides have been synthesized and have been attracting much attention. For example, $CaCu_3Mn_4O_{12}$ shows the large magnetoresistance at low magnetic fields³ and $CaCu_3Ti_4O_{12}$ has the large dielectric constant.⁴⁻⁶ $CaCu_3Ru_4O_{12}$ exhibits d -electron heavy-fermion behavior with electronic specific coefficient.⁷⁻⁹ Very recently, A-site ordered perovskite oxides $CaCu_3Fe_4O_{12}$ and $LaCu_3Fe_4O_{12}$ have been found to show interesting charge-ordering and/or charge-transfer phenomena.^{10,11}

Although the physical properties of the A-site ordered perovskite oxides have been attracting great interest, systematic understanding of their electronic structures is still lacking. In particular, the valence or the electronic configuration of the Cu ions in the A-site ordered perovskite oxides has not been studied using spectroscopic methods except $CaCu_3Ru_4O_{12}$, which is reported to have $Cu^{2+}(d^9)$.¹² In the present work, we report on a photoemission study of $CaCu_3Co_4O_{12}$ and $YCu_3Co_4O_{12}$ which are metallic and insulating, respectively. If the Cu valence is +2 as expected from the square planar coordination, the Co valence in $CaCu_3Co_4O_{12}$ is formally +4 and the system could be a Mott insulator. On the other hand, in $YCu_3Co_4O_{12}$, the Co valence is +3.75 and the system should be metallic or have some charge ordering. In spite of this expectation, $CaCu_3Co_4O_{12}$ shows a good metallic behav-

ior with large electronic density of states at the Fermi level and $YCu_3Co_4O_{12}$ shows an insulating behavior.¹³ The metallic behavior of $CaCu_3Co_4O_{12}$ is consistent with the recent band structure calculation.¹⁴ In addition, the electronic specific-heat coefficients of $CaCu_3Co_4O_{12}$ (Ref. 13) and $CaCu_3V_4O_{12}$ (Ref. 15) are moderately enhanced indicating that electron-electron and electron-phonon interactions play important roles to realize the correlated metallic states in A-site ordered perovskite oxides. The present photoemission study reveals that the Cu valence is formally +3 and the Cu ions has the d^9L configuration (L : an O $2p$ hole). This observation is consistent with the recent discovery of Cu^{3+} in $LaCu_3Fe_4O_{12}$ (Ref. 11) and resolves the above paradox on the valency and the band filling in $ACu_3Co_4O_{12}$. Also the nature of the correlated metallic state is investigated by photoemission spectroscopy.

II. EXPERIMENTS

The polycrystalline samples of $CaCu_3Co_4O_{12}$ and $YCu_3Co_4O_{12}$ were prepared by a solid-state reaction. Ca_2CuO_3 , CuO , Co_3O_4 , and Y_2O_3 were mixed and kept under 800 °C in air for 12 h. After that, they were packed into gold capsules and kept at 1000 °C under 9 GPa for 30 min with $KClO_4$. The electric resistivities of $CaCu_3Co_4O_{12}$ and $YCu_3Co_4O_{12}$ show metallic and insulating behaviors, respectively.¹³ The samples were confirmed to be stoichiometric using thermogravimetry analyses and x-ray diffraction measurements with synchrotron radiation.¹³ X-ray photoemission spectroscopy (XPS) measurements were carried out at 300 K using JPS9200 spectrometer (JEOL, Japan). Monochromatic Al $K\alpha$ (1486.6 eV) was used as an x-ray source. The pass energy of the electron analyzer was set to 10 eV. The total energy resolution including the x-ray source and the electron analyzer was about 0.6 eV. The binding energy was calibrated using the Fermi edge and the Au $4f$ core level of the gold reference sample. The ultraviolet photoemission spectroscopy (UPS) measurements were carried out at 30 K using SES-100 spectrometer (GammadataScienta, Sweden).

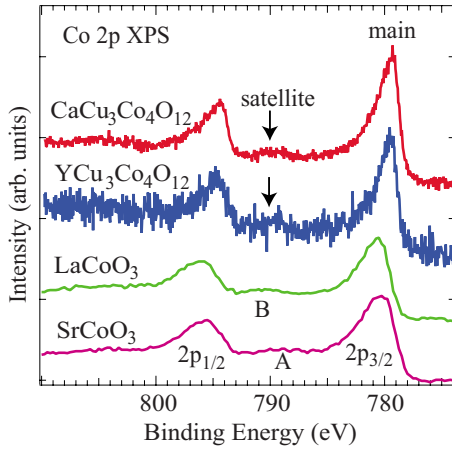


FIG. 1. (Color online). Co $2p$ core-level XPS spectra of $\text{CaCu}_3\text{Co}_4\text{O}_{12}$, and $\text{YCu}_3\text{Co}_4\text{O}_{12}$ compared with those of SrCoO_3 and LaCoO_3 . The satellite structures of SrCoO_3 and LaCoO_3 are labeled as A and B, respectively.

He I (21.2 eV) was used as a light source. The energy resolution was set to 30 meV. The binding energy was calibrated using the Fermi edge of the gold reference sample. Polycrystalline samples of $\text{ACu}_3\text{Co}_4\text{O}_{12}$ ($A=\text{Ca}$ and Y) was fractured *in situ* for the XPS and UPS measurements. The base pressure of the XPS and UPS chambers was $\sim 1 \times 10^{-7}$ Pa.

III. RESULTS AND DISCUSSION

In Fig. 1, the Co $2p$ core-level XPS results of $\text{CaCu}_3\text{Co}_4\text{O}_{12}$ and $\text{YCu}_3\text{Co}_4\text{O}_{12}$ are compared with those of LaCoO_3 and SrCoO_3 .¹⁶ Since the Co $2p$ binding energies of Co^{3+} in LaCoO_3 and Co^{4+} in SrCoO_3 are close to each other (~ 780 eV), it is difficult to identify the Co valence from the binding energy. However, the Co valence can be deduced by comparing the shape of satellite structure with those of LaCoO_3 and SrCoO_3 . The satellite structure of Co^{4+} (labeled as A) is flat compared to that of Co^{3+} (labeled as B). Since the difference between the satellite structure is reproduced by the CoO_6 cluster-model calculation,¹⁶ the satellite structure can be used to identify the Co valence. As shown in Fig. 1, the satellite spectral shapes of $\text{CaCu}_3\text{Co}_4\text{O}_{12}$ and $\text{YCu}_3\text{Co}_4\text{O}_{12}$ are similar to that of the Co^{3+} in LaCoO_3 . Therefore, it is reasonable to conclude that the electronic configuration of Co in $\text{CaCu}_3\text{Co}_4\text{O}_{12}$ and $\text{YCu}_3\text{Co}_4\text{O}_{12}$ is close to that of the Co^{3+} state in LaCoO_3 , namely, the low-spin d^6 configuration.

Figure 2 shows the Cu $2p$ core-level XPS spectra of $\text{CaCu}_3\text{Co}_4\text{O}_{12}$ and $\text{YCu}_3\text{Co}_4\text{O}_{12}$. The binding energies of the Cu $2p$ main peaks are ~ 934 eV in $\text{CaCu}_3\text{Co}_4\text{O}_{12}$ and $\text{YCu}_3\text{Co}_4\text{O}_{12}$. These values are similar to those of NaCuO_2 (Refs. 17 and 18) and LaCuO_3 (Ref. 19) where the Cu valence is formally +3 and the Cu ion takes the d^9L configuration that corresponds to the Zhang-Rice singlet state. Therefore, it is reasonable to conclude that, in $\text{CaCu}_3\text{Co}_4\text{O}_{12}$ and $\text{YCu}_3\text{Co}_4\text{O}_{12}$, the Cu valence is formally +3 and the d^9L configuration or the Zhang-Rice singlet state is realized. This conclusion is consistent with the Co $2p$ XPS result indicating that the Co valence is close to +3 and, consequently, the Cu

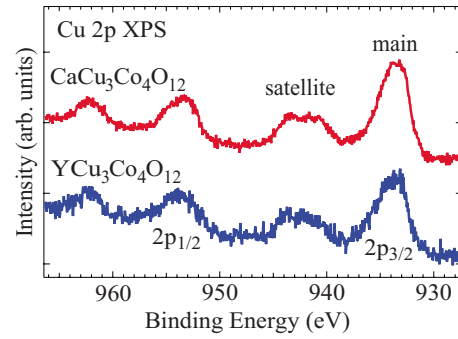


FIG. 2. (Color online). Cu $2p$ core-level XPS spectra of $\text{CaCu}_3\text{Co}_4\text{O}_{12}$, and $\text{YCu}_3\text{Co}_4\text{O}_{12}$.

valence is close to +3. The discovery of Cu^{3+} in $\text{CaCu}_3\text{Co}_4\text{O}_{12}$ and $\text{YCu}_3\text{Co}_4\text{O}_{12}$ is consistent with the recent discovery of Cu^{3+} in $\text{LaCu}_3\text{Fe}_4\text{O}_{12}$ (Ref. 11) and indicates that the square planar coordination of the Cu site is stabilized by the tilting of the CoO_6 octahedron instead of the Jahn-Teller effect of Cu^{2+} .

In these A-site ordered perovskite oxides, Cu^{2+} state with d^9 configuration is expected to be stable due to the square planar coordination. In $\text{CaCu}_3\text{Co}_4\text{O}_{12}$, if the Cu valence is +2, the Co valence is formally +4, and the system could be a Mott insulator. On the other hand in $\text{YCu}_3\text{Co}_4\text{O}_{12}$, the Cu valence is estimated to be +3.75 and the system should be metallic otherwise some charge orderings may open a band gap. In spite of the above expectation, transport measurements show that $\text{CaCu}_3\text{Co}_4\text{O}_{12}$ is a good metal with large electronic density of states at the Fermi level (E_F) and that $\text{YCu}_3\text{Co}_4\text{O}_{12}$ is an insulator.¹³ The above conclusion from the Co $2p$ and Cu $2p$ XPS results can resolve the paradox on the band filling. Assuming that the oxygen content of $\text{ACu}_3\text{Co}_4\text{O}_{12}$ is stoichiometric and that the band filling is controlled by the A-site cation, the Co valence is +3 with A-site cations of Y^{3+} and Cu^{3+} , consistent with the insulating behavior of $\text{YCu}_3\text{Co}_4\text{O}_{12}$. On the other hand, the Co valence is +3.25 with A-site cations of Ca^{2+} and Cu^{3+} . Therefore, $\text{CaCu}_3\text{Co}_4\text{O}_{12}$ can be viewed as a dope Mott insulator where the density of states near E_F is mainly constructed from the Co $3d$ orbitals strongly hybridized with the O $2p$ orbitals. In addition, since the Cu^{3+} site is dominated by the d^9L configuration, the Cu $3d$ component can be mixed into the Co $3d$ band via the O $2p$ component.

Figure 3 shows the O $1s$ core-level XPS spectra of $\text{CaCu}_3\text{Co}_4\text{O}_{12}$ and $\text{YCu}_3\text{Co}_4\text{O}_{12}$. The O $1s$ core-level peak of $\text{CaCu}_3\text{Co}_4\text{O}_{12}$ at ~ 528.5 eV is accompanied by the shoulder structure at ~ 529.4 eV and the broad satellite structure at $\sim 531-533$ eV. On the other hand, the O $1s$ core-level peak of $\text{YCu}_3\text{Co}_4\text{O}_{12}$ at ~ 528.9 eV is relatively sharp and is accompanied by the broad satellite structure at $\sim 531-533$ eV.

As predicted by the theoretical study by Okada and Kotani,²⁰ the satellite structure of O $1s$ XPS can provide direct evidence of the Zhang-Rice singlet ground state. However, the intensity of the satellite structure is much stronger than the theoretical prediction. Therefore, the satellite structure of O $1s$ XPS seen in the polycrystalline samples should be assigned to the surface contaminations. If clean surfaces of single crystals are available, then the surface contamina-

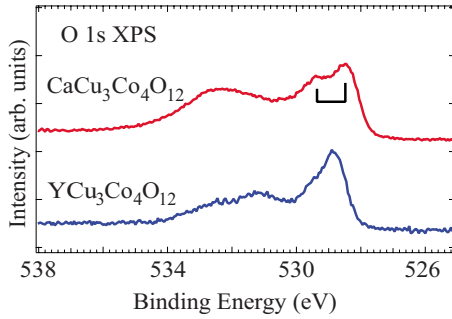


FIG. 3. (Color online). O $1s$ core-level XPS spectra of $\text{CaCu}_3\text{Co}_4\text{O}_{12}$, and $\text{YCu}_3\text{Co}_4\text{O}_{12}$. The broad structure at ~ 531 – 533 eV is derived from the surface contaminations.

tions can be removed and the intrinsic satellite structure can be observed as direct evidence of the Zhang-Rice singlet ground state. The O $1s$ satellite structure has two components at 531 and 532.5 eV. In $\text{CaCu}_3\text{Co}_4\text{O}_{12}$, the O $1s$ satellite is dominated by the component at 532.5 eV while the O $1s$ satellite in $\text{YCu}_3\text{Co}_4\text{O}_{12}$ shows the two components. Although it is difficult to identify the origins of the two components, the component at 532.5 eV is deduced to come from grain boundaries at the surface region and the component at 531 eV is probably due to oxygen loss from $\text{YCu}_3\text{Co}_4\text{O}_{12}$ at the surface region. If the grain boundary is thicker in $\text{CaCu}_3\text{Co}_4\text{O}_{12}$ than that in $\text{YCu}_3\text{Co}_4\text{O}_{12}$, the component at 532.5 eV can be dominant in $\text{CaCu}_3\text{Co}_4\text{O}_{12}$. With the thinner grain boundary, the oxygen loss from $\text{YCu}_3\text{Co}_4\text{O}_{12}$ at the surface region can take place more easily and the component at 531 eV can appear.

The energy splitting between the main peak and the shoulder structure in $\text{CaCu}_3\text{Co}_4\text{O}_{12}$ would be related to the difference between the oxygen ions involved in the CuO_4 square plane and those that are not involved. However, the energy splitting is absent in $\text{YCu}_3\text{Co}_4\text{O}_{12}$ that has the similar crystal structure to $\text{CaCu}_3\text{Co}_4\text{O}_{12}$. Another possible origin of the energy splitting in $\text{CaCu}_3\text{Co}_4\text{O}_{12}$ is the screening effect on the O $1s$ core hole due to the O $2p$ electrons. In the metallic $\text{CaCu}_3\text{Co}_4\text{O}_{12}$, the O $2p$ states can be involved in the electronic states near E_F and can screen the O $1s$ core hole to create the well-screened peak at ~ 528.5 eV and the poorly screened peak at ~ 529.4 eV. The significant O $2p$ contribution in the near- E_F electronic states is consistent with the interpretation of the Co $2p$ and Cu $2p$ core-level XPS spectra as discussed in the previous paragraphs.

Figure 4 shows the valence-band XPS spectra of $\text{CaCu}_3\text{Co}_4\text{O}_{12}$ and $\text{YCu}_3\text{Co}_4\text{O}_{12}$. As for the valence-band spectra, the peaks at ~ 1 and 3 eV are derived from the Co $3d$ and Cu $3d$ bands, respectively. The broad structure ranging from 3 to 8 eV can be attributed to the O $2p$ band hybridized with the Cu $3d$ and Co $3d$ orbitals. The overall valence-band structure of $\text{CaCu}_3\text{Co}_4\text{O}_{12}$ is very similar to that of $\text{YCu}_3\text{Co}_4\text{O}_{12}$ except the near- E_F region. The near- E_F spectral weight is strongly suppressed in $\text{YCu}_3\text{Co}_4\text{O}_{12}$ consistent with its insulating behavior. The near- E_F spectral weight is mainly derived from the Co $3d$ orbitals mixed with the O $2p$ and Cu $3d$ orbitals.

Figure 5 shows the UPS spectra of $\text{CaCu}_3\text{Co}_4\text{O}_{12}$ and $\text{YCu}_3\text{Co}_4\text{O}_{12}$ taken at 30 K. The spectral weight at E_F is

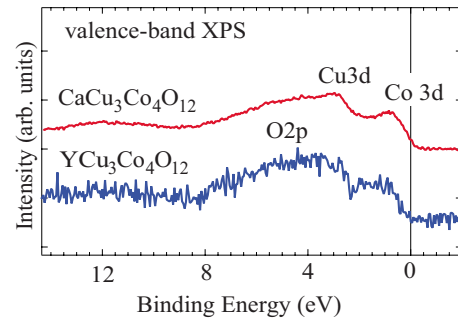


FIG. 4. (Color online). Valence-band XPS spectra of $\text{CaCu}_3\text{Co}_4\text{O}_{12}$, and $\text{YCu}_3\text{Co}_4\text{O}_{12}$ taken at 300 K with $h\nu = 1486.6$ eV. The spectral weight at E_F is strongly suppressed in $\text{YCu}_3\text{Co}_4\text{O}_{12}$ consistent with its insulating behavior.

substantial in metallic $\text{CaCu}_3\text{Co}_4\text{O}_{12}$ while it is suppressed in insulating $\text{YCu}_3\text{Co}_4\text{O}_{12}$. In $\text{YCu}_3\text{Co}_4\text{O}_{12}$, the Co $3d t_{2g}$ band is fully occupied by electrons and the top of Co $3d t_{2g}$ band is located at ~ 0.2 eV below E_F . The small amount of oxygen off-stoichiometry of $\text{YCu}_3\text{Co}_4\text{O}_{12}$ at the surface region created under the ultrahigh vacuum may responsible for the small spectral weight within the band gap. This is consistent with the interpretation of the satellite structure of O $1s$ XPS. In $\text{CaCu}_3\text{Co}_4\text{O}_{12}$, the Ca substitution for Y introduces holes into the Co $3d t_{2g}$ band which crosses E_F . In order to estimate the density of states at E_F from the experimental result, it is assumed that all the spectral weight near E_F is derived from the Co $3d t_{2g}$ band which is mainly constructed from the Co $3d$ orbitals hybridized with the O $2p$ and Cu $3d$ orbitals. We have extracted the Co $3d t_{2g}$ band by subtracting the tail of the O $2p$ contribution from the experimental result as shown in Fig. 6(a). Here, the tail of the O $2p$ contribution is approximated by the power-law function. The Co $2p$ XPS result shows that the Co ion is close to the low-spin d^6 configuration. Therefore, the number of Co t_{2g} electrons in a unit cell is $\sim 4 \times 6 = 24$. The integrated intensity of the obtained Co $3d t_{2g}$ band divided by 24 corresponds to the spectral area per t_{2g} electron. The intensity at E_F can be estimated from the symmetrized spectrum where the effect of Fermi-Dirac distribution function is removed as shown in Fig. 6(b). The intensity at E_F divided by the spectral area per t_{2g} electron and multiplied by Avogadro constant corresponds to the density of states $g(E_F)$ per formula unit. Assuming that the

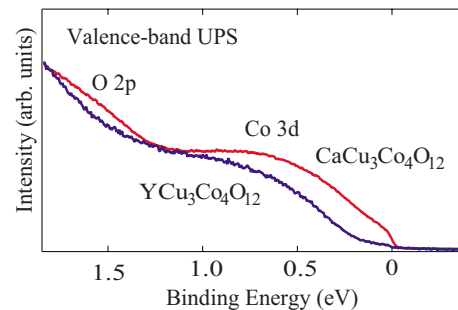


FIG. 5. (Color online). UPS spectra of $\text{CaCu}_3\text{Co}_4\text{O}_{12}$ and $\text{YCu}_3\text{Co}_4\text{O}_{12}$ taken at 30 K with $h\nu = 21.2$ eV. The spectral weight at E_F is substantial in $\text{CaCu}_3\text{Co}_4\text{O}_{12}$ while it is negligibly small in $\text{YCu}_3\text{Co}_4\text{O}_{12}$.

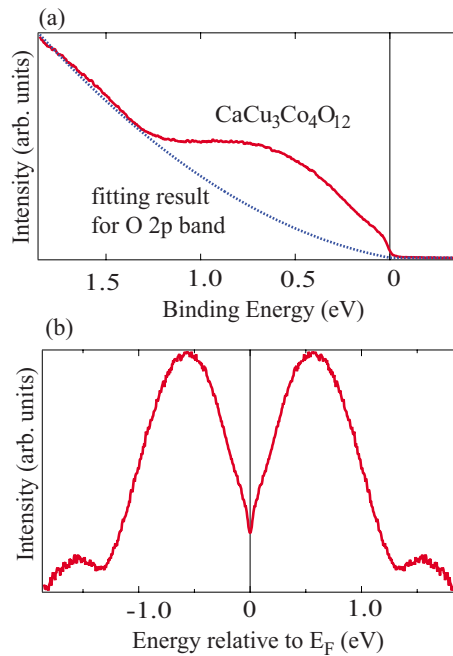


FIG. 6. (Color online). (a) O $2p$ band in the UPS spectrum of $\text{CaCu}_3\text{Co}_4\text{O}_{12}$ is approximated by the power-law function (dotted curve) and is subtracted from the UPS spectrum to extract the Co $3d t_{2g}$ band. (b) Symmetrized spectra of the Co $3d t_{2g}$ band in $\text{CaCu}_3\text{Co}_4\text{O}_{12}$.

renormalization factor z is unity, the electronic specific-heat coefficient $\gamma = \frac{\pi^2}{3} k_B^2 g(E_F)$ per formula unit is estimated to be 12 mJ/eV/K^2 . By comparing the estimated value with the experimental value of 160 mJ/mol/K^2 ,¹³ the inverse of the renormalization factor $1/z$ is ~ 13 which is probably due to the strong electron-electron and electron-phonon interactions.

IV. CONCLUSION

In summary, by means of photoemission spectroscopy, we have studied the electronic structure of A -site ordered perovskite oxides $\text{ACu}_3\text{Co}_4\text{O}_{12}$ ($A=\text{Ca}$ and Y) which are metallic for $A=\text{Ca}$ and insulating for $A=\text{Y}$. The photoemission study reveals that the Cu valence for $A=\text{Ca}$ and Y is formally +3 with the d^9L configuration (Zhang-Rice singlet) and that the Co valence for $A=\text{Ca}$ and Y are close to +3 with the low-spin d^6 configuration. In this electronic configuration, an O $2p$ hole is trapped by the Cu site and forms the d^9L configuration. If the O $2p$ hole is trapped by the Co site and forms the d^6L configuration, the formal valences of the Cu and Co sites can be viewed as +2 and +4 respectively. In $\text{ACu}_3\text{Co}_4\text{O}_{12}$, since the O $2p$ hole is trapped by the Cu site as concluded by the photoemission study, the formal valences of Co are +3.25 and +3 for $A=\text{Ca}$ and $A=\text{Y}$, respectively. This is consistent with the fact that $\text{CaCu}_3\text{Co}_4\text{O}_{12}$ is metallic and $\text{YCu}_3\text{Co}_4\text{O}_{12}$ is insulating. From the comparison between the photoemission spectra near the Fermi level and the electronic specific heat coefficient, the renormalization factor is estimated to be ~ 13 indicating that the electronic state near the Fermi level is strongly renormalized due to electron-electron and electron-phonon interactions.

ACKNOWLEDGMENTS

The authors would like to thank the valuable discussions with A. Fujimori, H. Wadati, and D. I. Khomskii. This work was supported by the Global COE program “the Physical Sciences Frontier” and the 21COE on the Kyoto Alliance for Chemistry from the Ministry of Education, Culture, Sports, Science, and Technology of Japan. It was also supported by Grants-in-Aid for Scientific Research from MEXT and from the Japan Society for the Promotion of Science (Grants No. 19GS0207 and No. 17105002).

- ¹M. Imada, A. Fujimori, and Y. Tokura, *Rev. Mod. Phys.* **70**, 1039 (1998).
- ²P. M. Woodward, *Acta Crystallogr. B* **53**, 32 (1997).
- ³Z. Zeng, M. Greenblatt, M. A. Subramanian, and M. Croft, *Phys. Rev. Lett.* **82**, 3164 (1999).
- ⁴M. A. Subramanian, D. Li, N. Duan, B. A. Reisner, and A. W. Sleight, *J. Solid State Chem.* **151**, 323 (2000).
- ⁵A. P. Ramirez, M. A. Subramanian, M. Gardel, G. Blumberg, D. Li, T. Vogt, and S. M. Shapiro, *Solid State Commun.* **115**, 217 (2000).
- ⁶C. C. Homes, T. Vogt, S. M. Shapiro, S. Wakimoto, and A. P. Ramirez, *Science* **293**, 673 (2001).
- ⁷W. Kobayashi, I. Terasaki, J. Takeya, I. Tsukada, and Y. Ando, *J. Phys. Soc. Jpn.* **73**, 2373 (2004).
- ⁸A. P. Ramirez, G. Lawes, D. Li, and M. A. Subramanian, *Solid State Commun.* **131**, 251 (2004).
- ⁹S. Tanaka, N. Shimazui, H. Takatsu, S. Yonezawa, and Y. Maeno, *J. Phys. Soc. Jpn.* **78**, 024706 (2009).
- ¹⁰I. Yamada, K. Takata, N. Hayashi, S. Shinohara, M. Azuma, S. Mori, S. Muranaka, Y. Shimakawa, and M. Takano, *Angew. Chem. Int. Ed.* **47**, 7032 (2008).
- ¹¹Y. W. Long, N. Hayashi, T. Saito, M. Azuma, S. Muranaka, and Y. Shimakawa, *Nature (London)* **458**, 60 (2009).
- ¹²T. T. Tran, K. Takubo, T. Mizokawa, W. Kobayashi, and I. Terasaki, *Phys. Rev. B* **73**, 193105 (2006).
- ¹³I. Yamada *et al.* (unpublished).
- ¹⁴H. P. Xiang, X. J. Liu, J. Meng, and Z. J. Wu, *J. Phys.: Condens. Matter* **21**, 045501 (2009).
- ¹⁵H. Shiraki, T. Saito, M. Azuma, and Y. Shimakawa, *J. Phys. Soc. Jpn.* **77**, 064705 (2008).
- ¹⁶T. Saitoh, T. Mizokawa, A. Fujimori, M. Abbate, Y. Takeda, and M. Takano, *Phys. Rev. B* **56**, 1290 (1997).
- ¹⁷T. Mizokawa, H. Namatame, A. Fujimori, K. Akeyama, H. Kondoh, H. Kuroda, and N. Kosugi, *Phys. Rev. Lett.* **67**, 1638 (1991).
- ¹⁸T. Mizokawa, A. Fujimori, H. Namatame, K. Akeyama, and N. Kosugi, *Phys. Rev. B* **49**, 7193 (1994).
- ¹⁹T. Mizokawa, A. Fujimori, H. Namatame, Y. Takeda, and M. Takano, *Phys. Rev. B* **57**, 9550 (1998).
- ²⁰K. Okada and A. Kotani, *J. Phys. Soc. Jpn.* **75**, 123703 (2006).